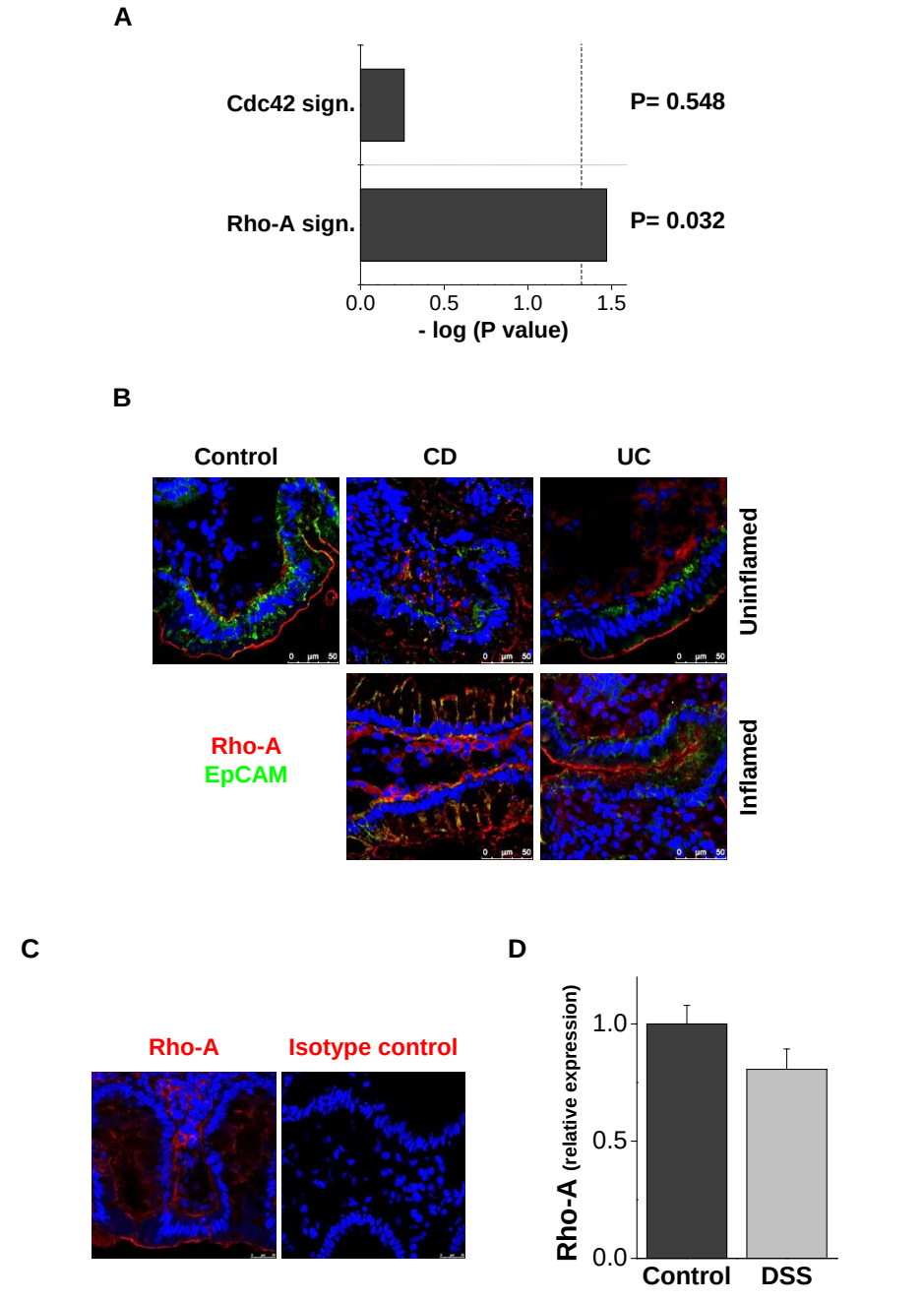

Supplementary Figure 1. Rho-A expression profile in human and murine colitis. **A.** Gene expression array in IECs isolated from 4 uninflamed and 5 inflamed gut areas from CD patients. Small GTPase pathways regulation, shown from GO profile. P-value was obtained by independent sample *t*- test (Ingenuity analysis). **B-C.** Rho-A immunostaining (red). **B.** Representative Rho-A immunostaining (red) in human biopsies, (lower magnification, corresponding to pictures shown in Figure 2B). Sections were counterstained with EpCAM (green) and Hoechst (blue). **C** Representative pictures showing specific staining **(left)** and isotype control **(right)**. Sections were counterstained with Hoechst (blue). **D**. Rho-A expression in IECs isolated from colon from DSS-exposed mice: mRNA expression measured by qPCR (Mean ± SEM, *n* = 4 per group). No statistical significance, independent sample *t*- test.

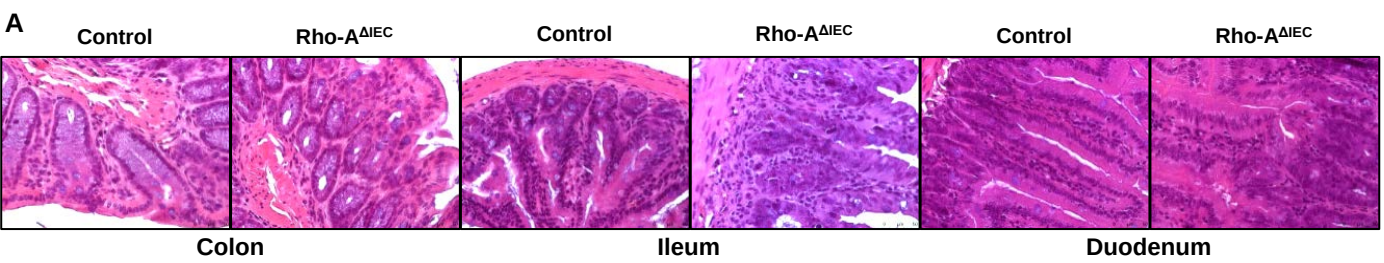

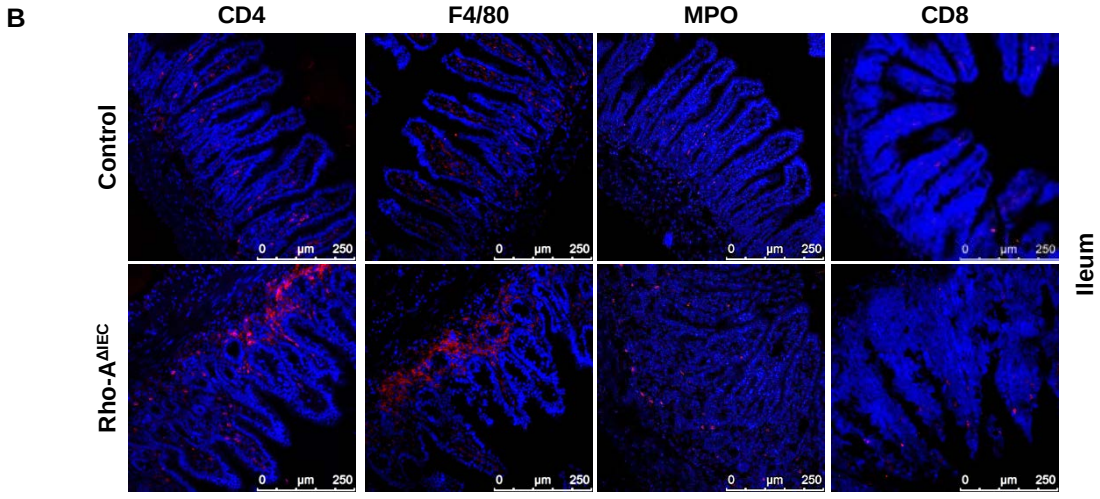

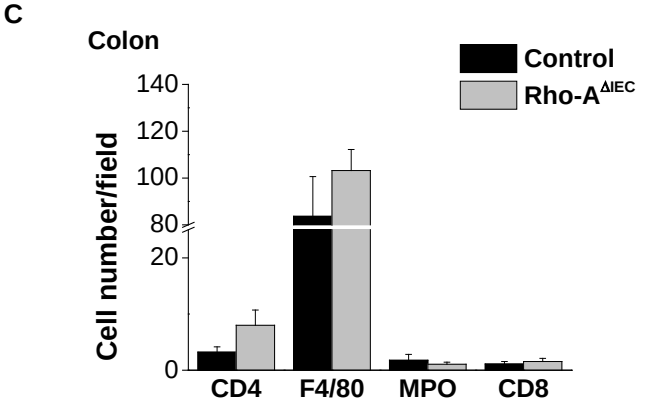

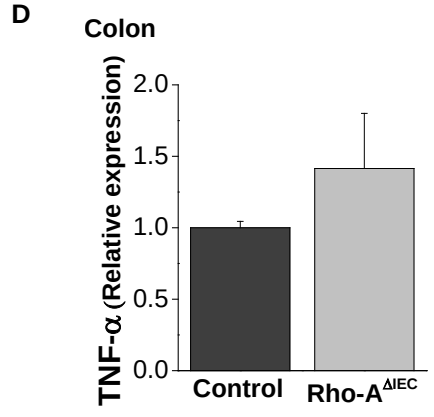

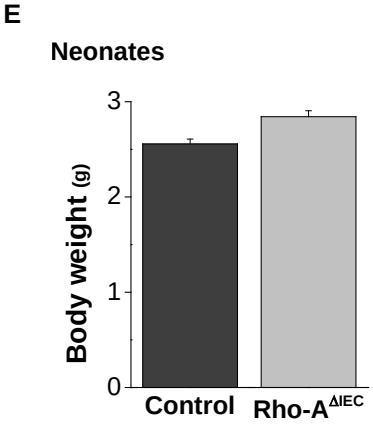

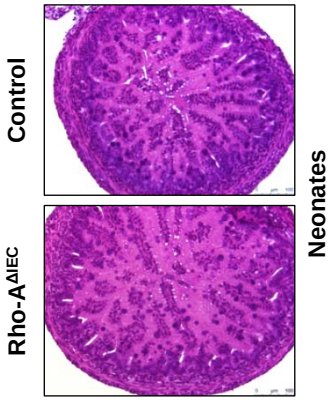

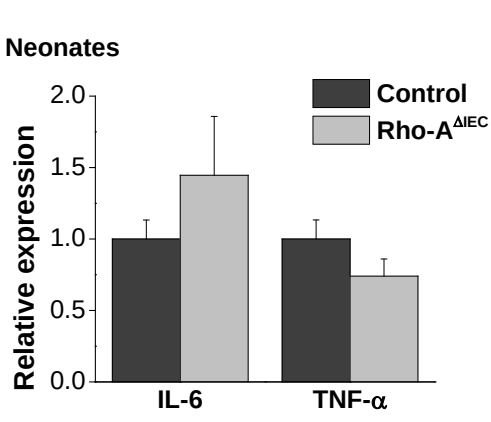

Supplementary Figure 2. Phenotype of Rho-A$^{\Delta IEC}$ mice. A. H&E pictures, (higher magnification, corresponding to pictures shown in Figure 3C). **B.** Representative pictures of CD4, F4/80, MPO and CD8 immunofluorescence stainings in ileum (corresponding quantification is shown in Figure 3D). **C.** Quantification of cell infiltration in colon (immunofluorescence staining). Mean values ± SEM (*n* = 6 per group). **D.** TNF-α expression in colon measured by qPCR. Mean values ± SEM (*n* = 6 per group). **E-G.** Phenotype of neonates from Rho-A$^{\Delta IEC}$ mice. **E.** Body weight (g). Mean values ± SEM of 10 mice. **F.** Representative pictures from H&E staining (8 samples**). G.** IL-6 and TNF-α in ileum measured by qPCR. Mean values ± SEM of 9 samples. No statistical significance; independent sample *t*-test in **C-E,G**.

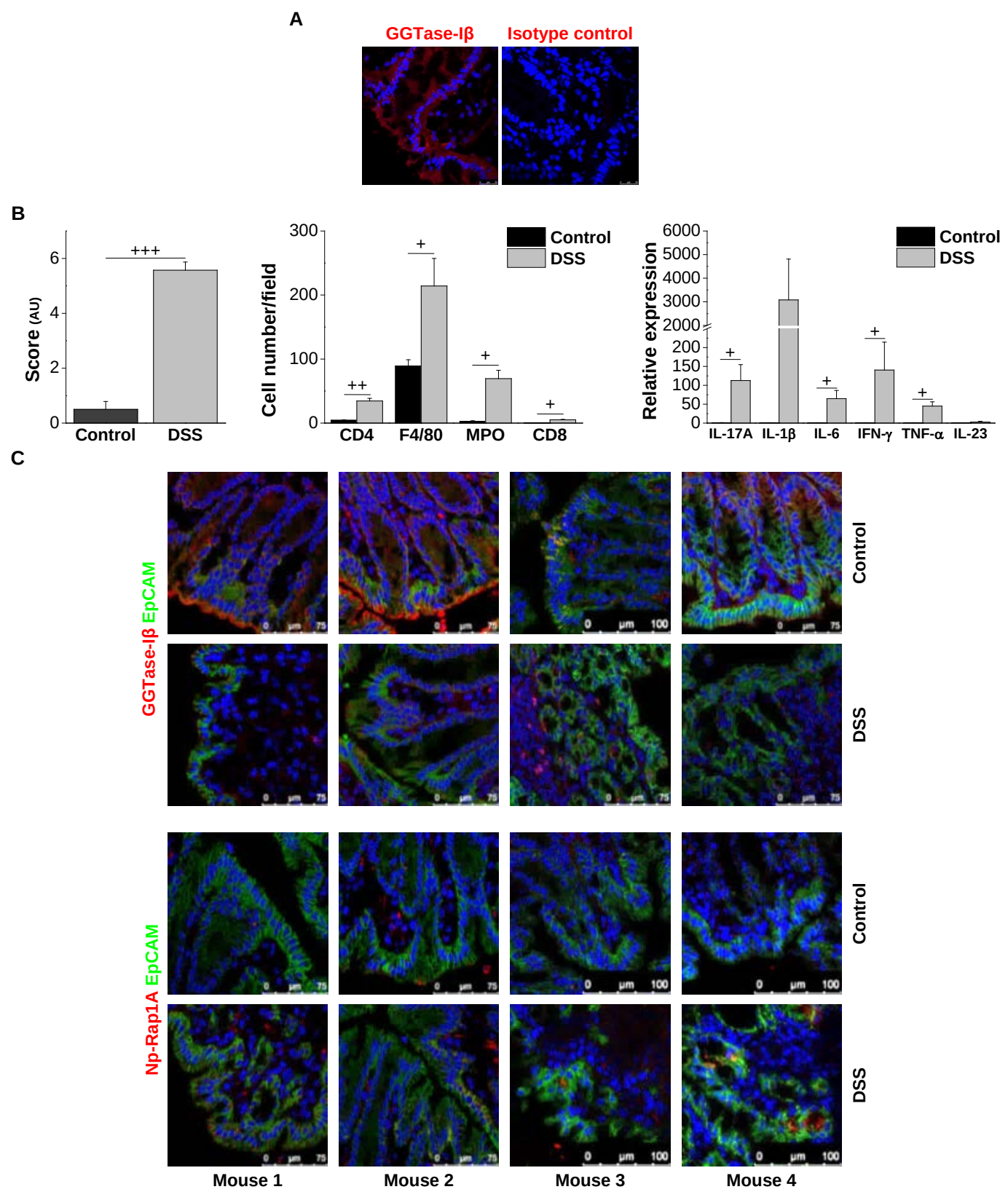

Supplementary Figure 3. GGTase-Iβ expression profile in DSS colitis in mice. A. GGTase-I immunostaining (red). Representative images showing specific staining **(left)** and isotype control **(right). B.** Quantification of colon inflammation in DSS-exposed mice: histological score (H&E staining) **(left)**; cell infiltration (immunofluorescence) **(middle)**; cytokine expression (qPCR) **(right)**. Mean values ± SEM (n = 6 per group). +$P \leq 0.05$; ++$P \leq 0.001$; +++$P \leq 0.0001$ vs. Control, independent sample t-test. **C.** GGTase-Iβ **(top)** and Np-Rap1A **(bottom)** immunostaining in colon from DSS-treated mice. Representative pictures from 4 independent experiments. Corresponding calculation of mean intensity of GGTase-Ib and Np-Rap1A is shown in Fig. 3D (n = 8 per group). Samples were counterstained with EpCAM (green) and Hoechst (blue).

A

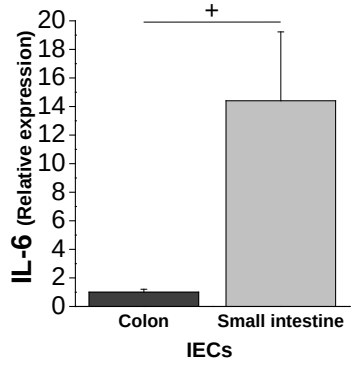

B

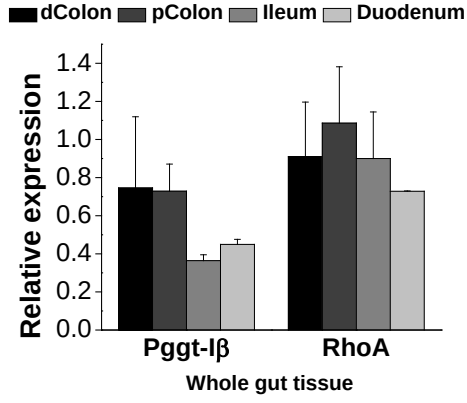

Supplementary Figure 4. Regional regulation of IL-6, GGTase-Iβ and Rho-A in intestine. A. IL-6 expression in isolated IECs from colon and small intestine from wild type mice (Mean ± SEM, *n* = 5 per group). +*P* ≤ 0.05 vs. Colon. **B.** GGTase-Iβ and Rho-A mRNA expression (mRNA) in different segments of whole gut tissue from wild type mice (Mean ± SEM, *n* = 3 per group). Independent sample *t*-test in **A,B**.

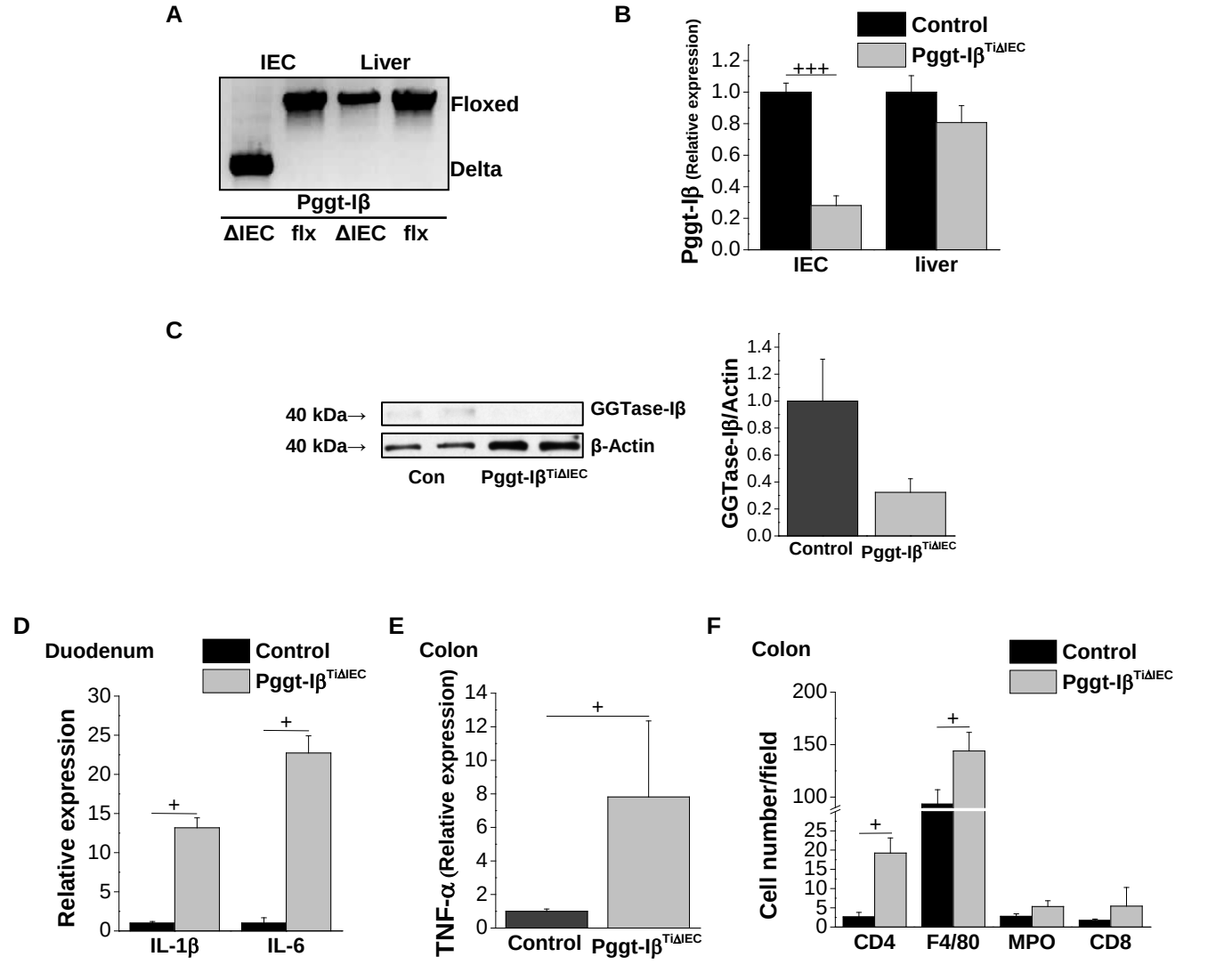

Supplementary Figure 5. Validation and phenotype of tamoxifen-induced GGTase-Iβ deletion (Pggt-Iβ^{TiΔIEC} mice). Pggt-Iβ^{TiΔIEC} mice were treated for three consecutive days with tamoxifen by i.p injection. Day 0 was defined as the day of the first tamoxifen injection. **A-C.** Validation of tamoxifen-induced GGTase-Iβ deletion (Pggt-Iβ^{TiΔIEC} mice). **A.** PCR of genomic DNA, detecting floxed (2000 bp) and Cre-recombinase deleted (Delta) allele (1350 bp) of *pggt1b* gene **(left)** (representative of three independent experiments). **B.** *pggt1b* mRNA levels measured by real time PCR. Mean ± SEM; *n*=5/group. **C.** Western blot of GGTase-Iβ in purified IECs, and quantification; two independent experiments (*n* = 4/group). **D.** IL-6 and IL-1β expression in duodenum measured by qPCR. Mean values ± SEM (*n* = 6 per group) **E-F.** Colon phenotype in Pggt-Iβ^{TiΔIEC} mice. Mean values ± SEM (*n* = 6/group). **E.** TNF-α expression in colon measured by qPCR. **F.** Quantification of cell infiltration in colon (immunofluorescence staining). +P ≤ 0.05. vs. Control in **D,E-F**. +++P ≤ 0.0001 vs. Control in **D**. Independent samples *t*-test in **B,C,D-F**.

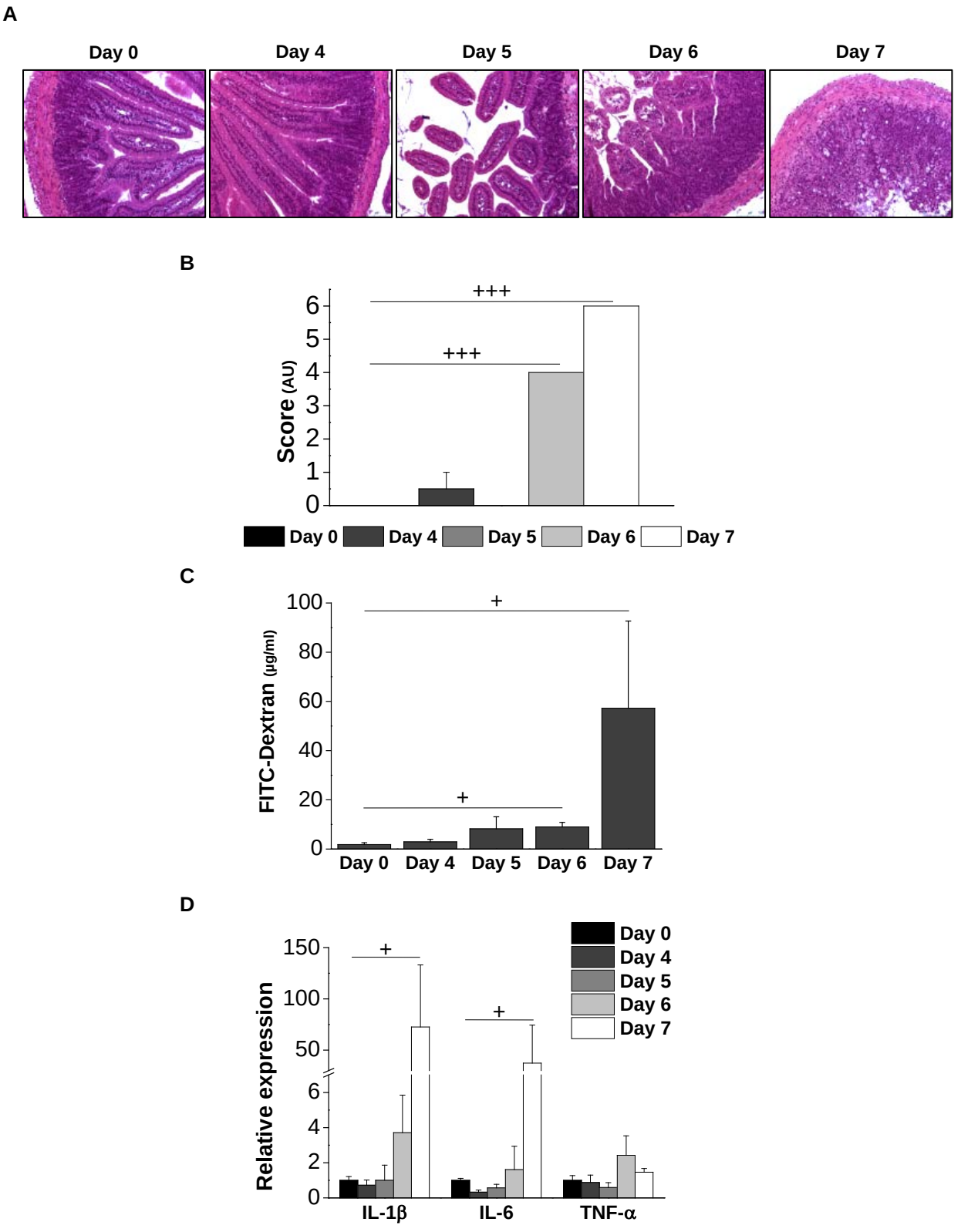

Supplementary Figure 6. Time course study of Pggt-Iβ ^{TiΔIEC} versus control mice. A. Representative histological images of small intestine (*n* = 13).. **B.** Score of tissue damage (histology). (Mean ± SEM, *n* = 13). **C.** Serum concentration of orally administered FITC-Dextran **D.** Cytokine expression measured by qPCR. (Mean ± SEM, *n*=13) in **A-D.** +P ≤ 0.05. vs. Day 0 in **C-D**. +++P ≤ 0.0001. in **B.** One-way ANOVA with LSD multiple comparisons test in **B-D**.

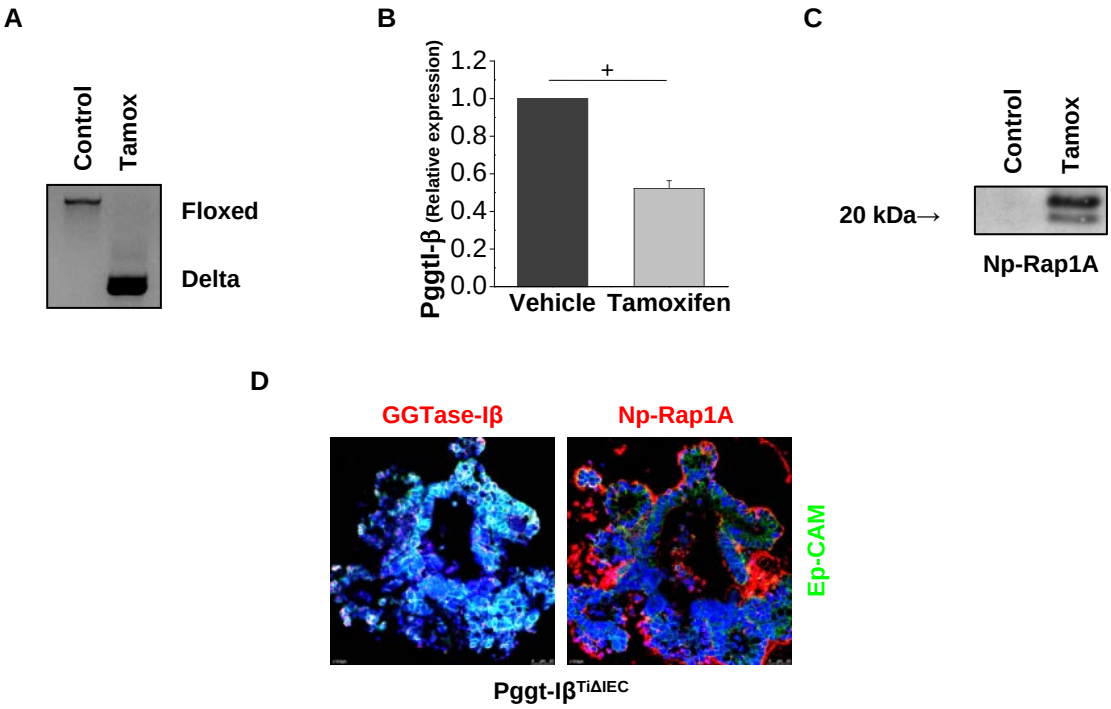

Supplementary Figure 7. Small intestinal crypts isolated from control and Pggt-IβTiΔIEC mice and treated in vitro with tamoxifen. A. PCR of genomic DNA detecting floxed allele (2000 bp) and Cre-recombinase deleted (Delta) allele (1350 bp) of *pggt1b* gene. **B.** GGTase-Iβ mRNA expression levels were detected by qPCR. Mean ± SEM, *n* = 2 samples/group. **C.** Detection of non-prenylated form of Rap1A (np-Rap1A) by Western Blot. **D.** GGTase-I **(left)** or np-Rap1A **(right)** staining in red, counterstained with Ep-CAM (green) and Hoechst (blue) in Pggt-IβTiΔIEC organoids. Three independent experiments in **A,C-D**. +P ≤ 0.05. vs. Vehicle, independent samples *t*-test in **B**.

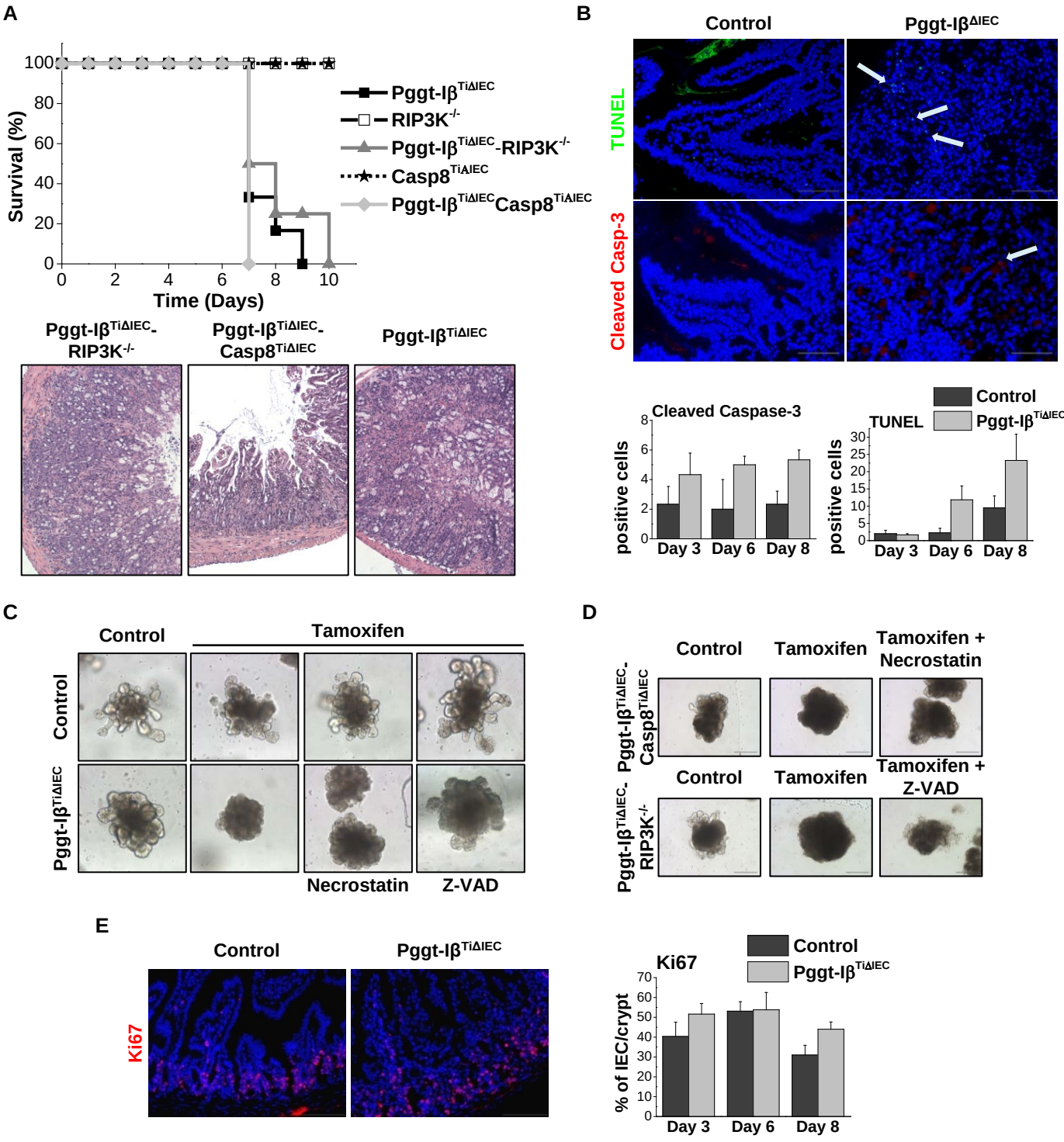

Supplementary Figure 8. Cellular mechanism in Pggt-IβTiΔIEC mice A. Survival of Pggt-IβTiΔIEC versus Pggt-IβTiΔIEC, Casp8TiΔIEC and Pggt-Iβ TiΔIECRIP3K-/- mice (*n* = 3/group) **(top)**. Histological analysis of duodenum from Pggt-IβTiΔIEC, Pggt-IβTiΔIECCasp8 TiΔIEC and Pggt-Iβ TiΔIECRIP3K-/- mice after tamoxifen treatment (pictures are representative of three independent experiments) **(bottom)**. **B.** Representative TUNEL (green) and cleaved caspase-3 (red) staining of duodenum cross-sections from Control and Pggt-IβTiΔIEC mice on day 8 after tamoxifen treatment **(top).** Quantification of TUNEL and caspase-3 positive cells **(bottom)**. Mean ± SEM, *n* = 3/group. **C.** Development of organoids generated from crypts isolated from small intestine of control and Pggt-IβTiΔIEC mice. Organoids were treated in vitro with tamoxifen alone or in combination with Necrostatin-1 or z-VAD, respectively. Pictures are representatives of two experiments. **D.** Development of organoids generated from small intestine crypts of of Pggt-IβTiΔIECCasp8 TiΔIEC and Pggt-IβTiΔIECRIP3K-/- mice, treated with tamoxifen in vitro alone or in combination with Necrostatin-1 or z-VAD. Pictures are representative of two experiments. **E.** Representative ki67 immunostaining (red) on duodenum cross-sections (two independent experiments) **(left).** Quantification of Ki67 positive cells/crypt in small intestine of control and Pggt-IβTiΔIEC mice. Mean ± SEM of *n* = 4 crypts/group **(right).** Sections were counterstained with Hoechst (blue) in **B,E**. No statistical significance, independent samples *t*-test in **B,E.**

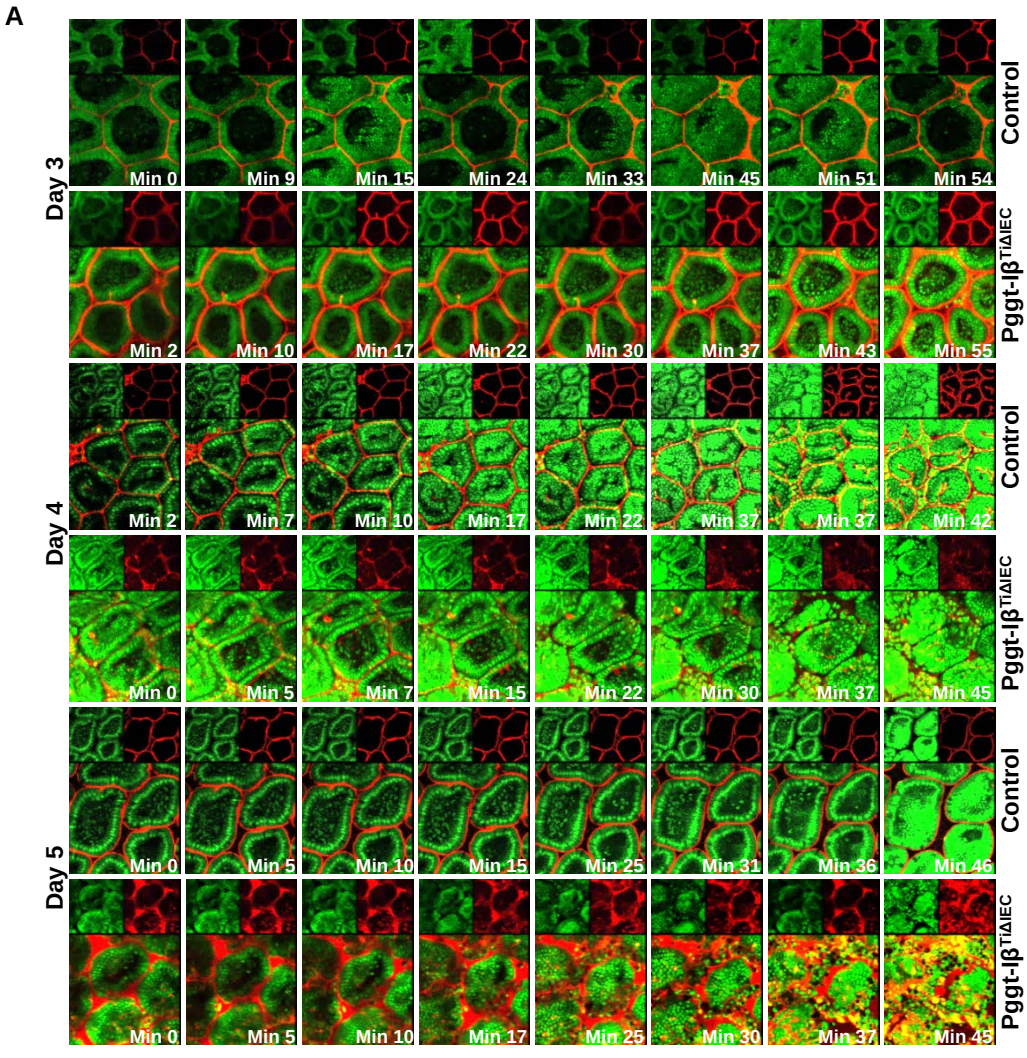

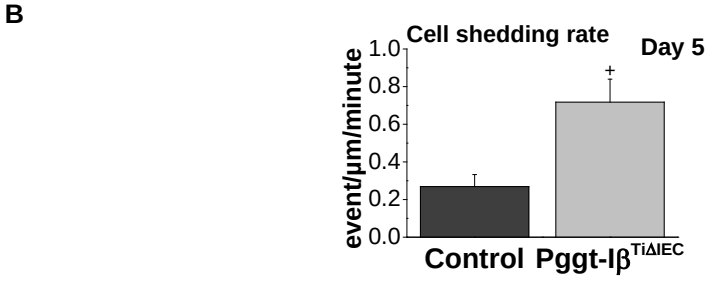

Supplementary Figure 9. Epithelial integrity in GGTase-I deficient epithelium (live imaging). A. In vivo imaging of villus tips in control and Pggt-I$\beta^{TiΔIEC}$ mice over time after starting tamoxifen treatment. Tissue was stained with acriflavine (green) and luminal Rhodamine-Dextran (red) in order to show the epithelial leakage. Pictures were taken by confocal microscopy (63x magnification). Pictures are representative of two independent experiments **B.** Cell shedding rate quantification of villus tips from control and Pggt-I$\beta^{TiΔIEC}$ mice. Data are expressed as Mean ± SEM of 5 villi (events/µm of basal membrane/minute). +P ≤ 0.05. vs. Control, independent samples *t*-test in **B**.

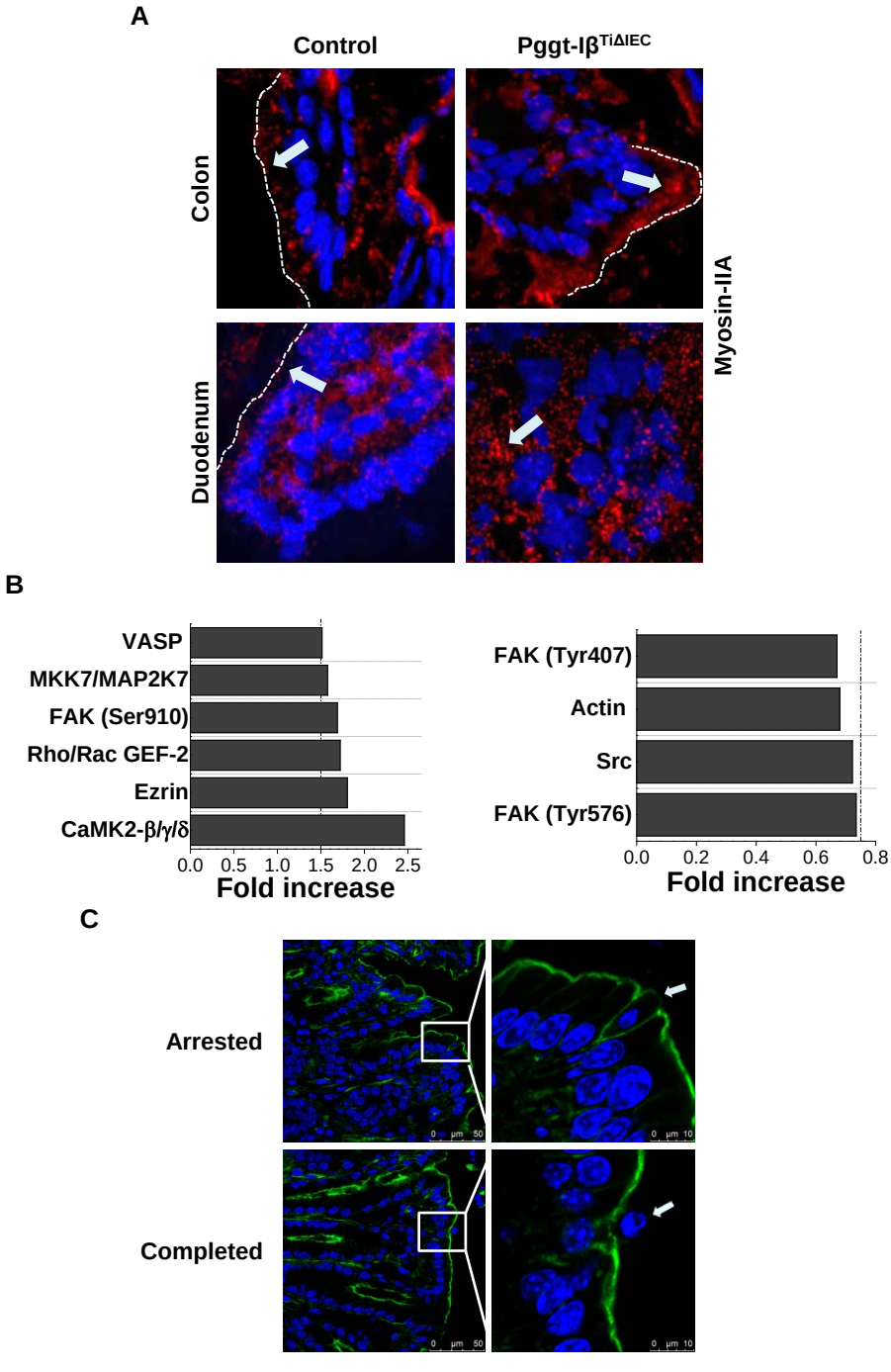

Supplementary Figure 10. Cytoskeleton rearrangement and arresting of cell shedding. A. Representative pictures (three independent experiments) from myosin-IIA staining (red) in control and Pggt-Iβ^{TiΔIEC} mice. Arrows indicate localization of myosin-IIA; and dotted lines indicate the apical membrane. **B.** Phosphorylation of cytoskeleton-related proteins up- or downstream of Rho-A: increased **(left)**, and decreased phosphorylation **(right)**. Fold increase; *n* = 3 control mice, and *n* = 3 Pggt-Iβ^{TiΔIEC} mice. Independent samples *t*-test. **C.** Representative pictures of phalloidin staining of F-actin fibers in colon: arrested **(top)** versus completed **(bottom)** cell shedding events. Arrested shedding events show redistribution of actin fibers leading to funnel-like structures; the cytosol as well as the nucleus is still part of the monolayer. After completion of cell shedding, the cell is extruded, and the nucleus appears in the lumen. Nuclei were counterstained with Hoechst in **A-C**.

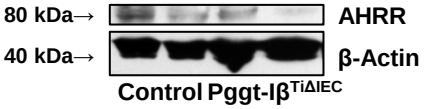

Supplementary Figure 11. AHR signaling in IECs from Pggt-IβTiΔIEC mice. Western blot detecting AHRR expression within IECs isolated from control and Pggt-IβTiΔIEC mice on day 6 after tamoxifen treatment. The same samples are shown in Figure 6A. Blots are representative of two experiments.

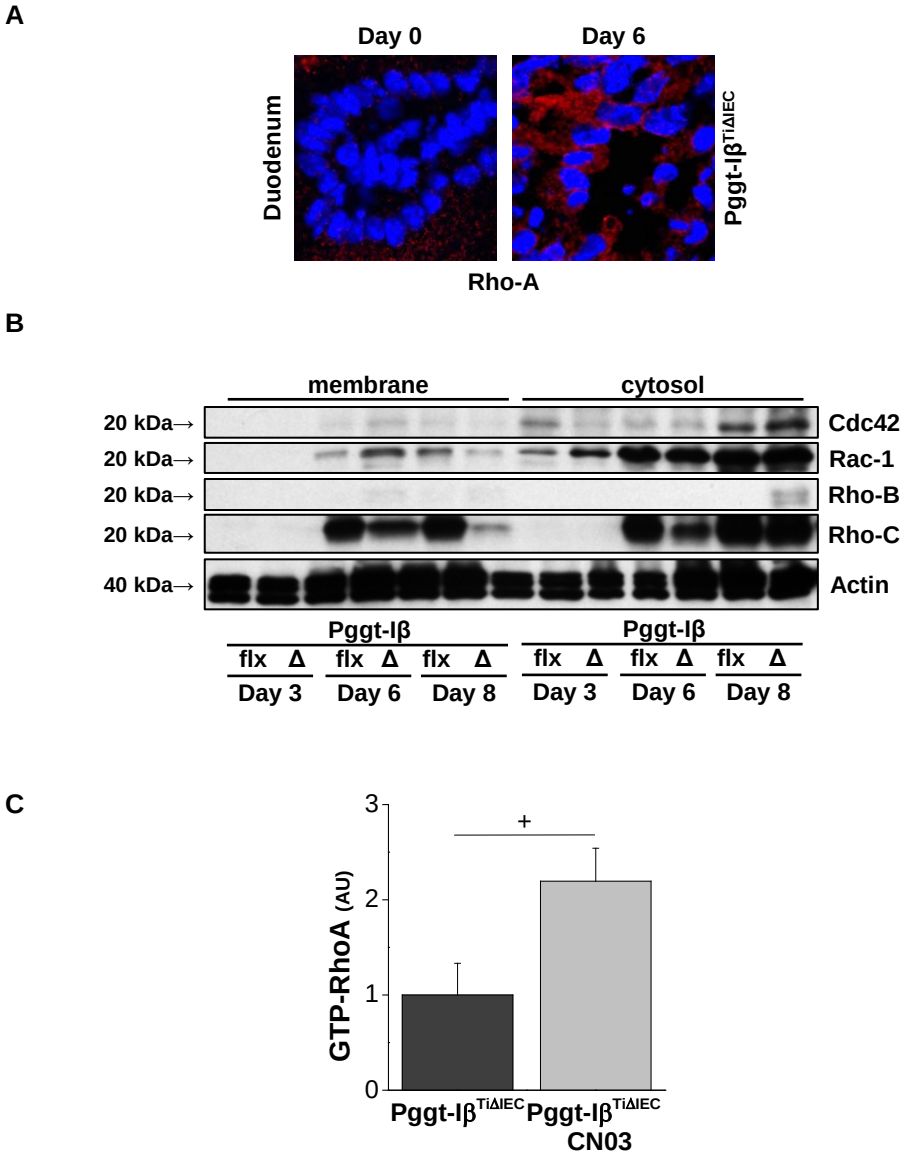

Supplementary Figure 12. Rho small GTPases in IECs from Pggt-IβTiΔIEC mice and CN03 treated mice. A. Rho-A immunostaining of duodenum from Pggt-IβTiΔIEC mice before and after treatment with tamoxifen. Pictures are representative of two independent experiments. Nuclei were counterstained with Hoechst (blue). **B.** Subcellular localization of small GTPases belonging to Rho family. Protein content in membrane and cytosol fraction was measured by Western blot (Cdc42, Rac-1, Rho-B, Rho-C); blots are representative of two experiments. **C.** GTP-bound Rho-A in IECs from Pggt-IβTiΔIEC mice with and without CN03 treatment.Mean ± SEM, *n*=9, +P≤0.0.5 vs. Pggt-IβTiΔIEC mice , independent sample *t*-test.

Supplemental Information

Supplementary tables

Supplementary Table 1

Clinical information from patients included in the gene expression array

ID	Group	Gender	Age	Disease	Location	Treatment	Disease activity (Endoscopy)	Disease course (duration)
1	Uninflamed	m	71	Healthy area from CD	Ileo-colonic	5-ASA Azathioprine Adalimumab Steroids	N/A	10 years
2	Uninflamed	f	53	Healthy area from CD	Ileo-colonic	5-ASA Prednisone Adalimumab Infliximab Azathioprine	N/A	5 years
3	Uninflamed	f	40	Healthy area from CD	Ileal	Budesonide 5-ASA	N/A	13 years
	Inflamed			Inflamed area from CD			Severe	
4	Uninflamed	m	53	Healthy area from CD	Ileal	5-ASA	N/A	1 years
	Inflamed			Inflamed area from CD			Severe	
5	Inflamed	f	51	Inflamed area from CD	Ileal	Prednisone 5-ASA	Severe	8 years
6	Inflamed	m	71	Inflamed area from CD	Ileal	Budesonide 5-ASA Adalimumab	Severe	27 years
7	Inflamed	m	27	Inflamed area from CD	Ileal	5-ASA Prednisone	Moderate	3 years

Supplementary Table 1 describes relevant clinical parameters of patients included in the gene expression array.

N/A = not applicable.

Supplementary Table 2

Clinical information from patients included in the qPCR analysis of Rho-A

Patient ID	Group	Gender	Age	Disease	Location	IBD treatment	Disease activity (Histology)	Disease course (Duration)
1	Control	female	83	Sigma diverticulitis	Sigmoid colon	N/A	N/A	N/A
2	Control	male	64	Tumor	Colon ascendens	N/A	N/A	N/A
3	Control	male	58	Tumor	Sigmoid colon	N/A	N/A	N/A
4	Control	female	73	Tumor	Rectum	N/A	N/A	N/A
5	CD-Uninflamed	male	42	CD	Ileum	Azathioprine	None	17 years
	CD-Inflamed				Ileum		Severe	
6	CD-Uninflamed	male	33	CD	Ileum	Azathioprine Prednisolon	None	16 years
	CD-Inflamed				Ileum		Moderate	
7	CD-Uninflamed	male	19	CD	Terminal Ileum	Infliximab	None	6 years
	CD-Inflamed				Terminal Ileum		Moderate	
8	CD-Uninflamed	female	84	CD	Ileum	N.d.a	None	N.d.a
	CD-Inflamed				Ileum		N.d.a	
9	UC-Uninflamed	male	52	CD	Terminal Ileum	Mesalazine	None	36 years
	UC-Inflamed				Terminal Ileum		Moderate	
10	UC-Uninflamed	male	25	UC	Left colic flexure	Prednisolon Anti-TNF-α (refractory)	Mild	13 years
	UC-Inflamed				Colon ascendens		Severe	
11	UC-Uninflamed	male	33	UC	Rectum	Golimumab	None	5 years
	UC-Inflamed				Rectum		Severe	
12	UC-Uninflamed	female	41	UC Tumor	Sigmoid Rectum	N.d.a	None	N.d.a
	UC-Inflamed				Rectum		N.d.a	
13	UC-Uninflamed	male	58	UC	Colon	N.d.a	None	N.d.a
	UC-Inflamed				Colon		N.d.a	

Supplementary Table 2 describes available and relevant clinical parameters of patients included in qPCR analyses (Rho-A). Classification of inflammation status (uninflamed versus inflamed) was based on macroscopic tissue evaluation after surgery performed by a pathologist. Non-IBD tumor patients were included as control collective; tumor-free tissue was analyzed. One of included UC patients (ID 12) was also suffering from intestinal

tumor; only tumor-free tissue was analyzed.As indicated, some data were either not available (N.d.a) or not applicable (N/A).

Supplementary Table 3

Clinical information from patients included in the immunofluorescence analysis

Patient ID	Group	Gender	Age	Disease	Location	IBD Treatment	Disease activity (Histology)	Disease duration (years)	Protein
1	Control	f	73	Tumor	Colon ascendens	N/A	N/A	N/A	Pggt-Iβ Rho-A
2	Control	m	71	Tumor	Coecum	N/A	N/A	N/A	Rho-A
3	Control	m	56	Tumor	Rectum	N/A	N/A	N/A	Rho-A
4	Control	m	63	Tumor	Terminal Ileum	N/A	N/A	N/A	Rho-A
5	Control	f	70	Tumor	Ileum	N/A	N/A	N/A	Rho-A
6	Control	m	68	Tumor	N.d.a	N/A	N/A	N/A	Pggt-Iβ
7	Control	m	62	Tumor	Colon ascendens	N/A	N/A	N/A	Pggt-Iβ
8	Control	f	48	Tumor	Rectum	N/A	N/A	N/A	Pggt-Iβ
9	Control	m	72	Tumor	Colon ascendens	N/A	N/A	N/A	Pggt-Iβ
10	Control	m	61	Tumor	Colon transversum	N/A	N/A	N/A	Pggt-Iβ
11	IBD-Uninflamed	m	14	CD	Ileocecal	N.d.a	None	N.d.a	Rho-A
12	IBD-Uninflamed	m	58	CD	Terminal Ileum	Prednisolon	None	3	Pggt-Iβ
13	IBD-Uninflamed	f	36	CD	Ileum	Prednisolon	Mild	1	Pggt-Iβ
14	IBD-Uninflamed	f	65	CD	N.d.a	N.d.a	None	N.d.a	Pggt-Iβ
15	CD-Uninflamed	m	41	CD	Colon	Infliximab	None	17	Rho-A
	CD-Inflamed				Small intestine		Moderate		
16	CD-Uninflamed	m	22	CD	Ileum	Adalimumab	None	4	Rho-A Pggt-Iβ
	CD-Inflamed				Ileum		Moderate		
17	CD-Uninflamed	f	47	CD	Small intestine	N.d.a	None	N.d.a	Rho-A
	CD-Inflamed				Small intestine		Moderate		
18	CD-Uninflamed	m	47	CD Tumor	Small intestine	N.d.a	None	N.d.a	Pggt-Iβ
	CD-Inflamed				Small intestine		Moderate		
19	CD-Uninflamed	m	42	CD	Small intestine	N.d.a	None	N.d.a	Pggt-Iβ
	CD-Inflamed				Small intestine		Moderate		
20	CD-Inflamed	f	43	CD	Small intestine	N.d.a	Moderate	10	Pggt-Iβ
21	CD-Inflamed	m	21	CD	Small intestine	Budesonide	Moderate	1	Pggt-Iβ

22	CD-Inflamed	m	47	CD	Colon ascendens	N.d.a	Severe	N.d.a	Pggt-Iβ
23	CD-Inflamed	N.d.a	N.d.a	CD	N.d.a	N.d.a	Severe	N.d.a	Pggt-Iβ
24	UC-Uninflamed	m	25	UC	Colon ascendens	Adalimumab	None	3	Rho-A
	UC-Inflamed				Sigmoid colon		Severe		
25	UC-Uninflamed	m	26	UC	Left colic flexure	Prednisolon	None	3	Rho-A
	UC-Inflamed				Colon ascendens		Severe		
26	UC-Uninflamed	m	33	UC	Rectum	Adalimumab	None	5	Rho-A
	UC-Inflamed				Colon ascendens		Severe		
27	UC-Uninflamed	m	27	UC	Ileum	Tacrolimus Prednisolon Mesalazine	None	5	Pggt-Iβ
	UC-Inflamed				Colon		Mild		
28	UC-Inflamed	f	46	UC	Colon	N.d.a	Moderate	N.d.a	Pggt-Iβ
29	UC-Inflamed	m	35	UC	Colon	None	Moderate	16	Pggt-Iβ
30	UC-Inflamed	m	76	UC	Colon	Infliximab (refractory)	Severe	N.d.a	Pggt-Iβ
31	UC-Inflamed	f	26	UC	Colon	N.d.a	Severe	N.d.a	Pggt-Iβ

Supplementary Table 3 describes available and relevant clinical parameters of patients included in qPCR analyses. Classification of inflammation status (uninflamed versus inflamed) was based on macroscopic tissue evaluation after surgery performed by a pathologist. Non-IBD tumor patients were included as control collective; tumor-free tissue was analyzed. One of included CD patients (ID 18) was also suffering from intestinal tumor; only tumor-free tissue was analyzed. Indicated duration of disease described time since initial diagnosis. As indicated, some data were either not available (no data available = n.d.a) or not applicable (N/A).

Supplementary Table 4

Clinical information from patients included in the qPCR analysis of GGTase-Iβ

Patient ID	Group	Gender	Age	Disease	Location	IBD treatment	Disease activity (Histology)	Disease course (Duration)
1	Control	male	64	Tumor	Colon ascendens	N/A	N/A	N/A
2	Control	male	89	Tumor	Colon ascendens	N/A	N/A	N/A
3	Control	female	73	Tumor	Rectum	N/A	N/A	N/A
4	CD-Uninflamed	male	33	CD	Ileum	Azathioprine	None	16 years
	CD-Inflamed				Ileum		N.d.a	
5	CD-Uninflamed	male	40	CD	Ileum	None	Mild	18 years
	CD-Inflamed				Ileum		Severe	
6	CD-Uninflamed	male	42	CD	Ileum	Azathioprine	None	17 years
	CD-Inflamed				Ileum		Severe	
7	UC-Uninflamed	male	58	UC	Colon	N.d.a	None	N.d.a
	UC-Inflamed				Colon		N.d.a	
8	UC-Uninflamed	female	26	UC	Colon ascendens	Adalimumab	None	7 years
	UC-Inflamed				Sigmoid colon		Moderate	
9	UC-Uninflamed	male	26	UC	Left colic flexure	Prednisolon	None	13 years
	UC-Inflamed				Colon ascendens		Severe	
10	UC-Uninflamed	male	33	UC	Rectum	Golimumab	None	5 years
	UC-Inflamed				Colon ascendens		Severe	

Supplementary Table 4 describes available and relevant clinical parameters of patients included in qPCR analyses (GGTase-Iβ). Classification of inflammation status (uninflamed versus inflamed) was based on macroscopic tissue evaluation after surgery performed by a pathologist. Non-IBD tumor patients were included as control collective; tumor-free tissue was analyzed. As indicated, some data were either not available (N.d.a) or not applicable (N/A).

Supplementary Table 5

Protein and gene expression analysis in IECs from Pggt-Iβ$^{\Delta IEC}$ mice.

Protein and gene expression analysis in IECs from Pggt-Iβ^{TiΔIEC} mice				
TOP regulated genes / proteins	**Gene expression (fold change)**		**Proteomics (fold change)**	
Cellular function	**UP**	**DOWN**	**UP**	**DOWN**
Cell cycle/proliferation/ death	TNFRSF12A (6.426)	G0S2 (14.720)		
	BTC (5,670)			
	RIPK3 (5.685)	FASLG (12.948)		
	GCH1 (5.035)			
	LATS1 (4.941)	F2R (11.193)		
	ID4 (3,787)			
Cytoskeleton / morphology / adhesion	CAPG (10.401)	ITGAE (11.811)	KRT81 (32.544)	PIGR (6.650)
	CAPN2 (4.324)		KRT31 (9.691)	TRIO (6.215)
	CAP1 (4.129)	F2R (11.193	Krt85 (9.111)	TUBB4A (6.002)
	Tmsb4x (3.813)		CAPG (8.416)	
Others (metabolism, protein interaction, non epithelial cell pathways)		SLC2A3 (24.156)	PAGP1 (6.125)	FBP1 (13.978)
		CD3G (20.920)	UMPS (7.406)	ARG2 (8.016)
		CD244 (17.074)	CELA1 (4.897)	CAT (5.791)
		CD7 (15.502)	CELA3B (4.453)	GALM (5.576)
		IL2RB (14.075)	REG1A (4.396)	Gstm3 (5.340)
		IKZF3 (13.514)	OASL (4.376)	UBE2D1 (4.969)
				EPHX2 (4.849)

Supplementary Table 5 summarizes the top 10 regulated proteins and genes.